Development 111, 509-522 (1991)
Printed in Great Britain © The Company of Biologists Limited 1991

Analysis of distribution patterns of gap junctions during development of embryonic chick facial primordia and brain

ROBERT MINKOFF[1,*], SUSAN B. PARKER[1] and ELLIOT L. HERTZBERG[2]

[1]*University of Texas Health Science Center at Houston, Department of Orthodontics, Dental Branch, Houston, Texas 77030, USA*
[2]*Albert Einstein College of Medicine, Department of Neuroscience and of Anatomy and Structural Biology, Bronx, NY, USA*

* Author for correspondence

Summary

Gap junction distribution in the facial primordia of chick embryos at the time of primary palate formation was studied employing indirect immunofluorescence localization with antibodies to gap junction proteins initially identified in rat liver ($27\times10^3 M_r$, connexin 32) and heart ($43\times10^3 M_r$, connexin 43). Immunolocalization with antibodies to the rat liver gap junction protein ($27\times10^3 M_r$) demonstrated a ubiquitous and uniform distribution in all regions of the epithelium and mesenchyme except the nasal placode. In the placodal epithelium, a unique non-random distribution was found characterized by two zones: a very heavy concentration of signal in the superficial layer of cells adjacent to the exterior surface and a region devoid of detectable signal in the interior cell layer adjacent to the mesenchyme. This pattern was seen during all stages of placode invagination that were examined. The separation of gap junctions in distinct cell layers was unique to the nasal placode, and was not found in any other region of the developing primary palate. One other tissue was found that exhibited this pattern – the developing neural epithelium of the brain and retina. These observations suggest the presence of region-specific signaling mechanisms and, possibly, an impedance of cell communication among subpopulations of cells in these structures at critical stages of development. Immunolocalization with antibodies to the 'heart' $43\times10^3 M_r$ gap junction protein also revealed the presence of gap junction protein in facial primordia and neural epithelium. A non-uniform distribution of immunoreactivity was also observed for connexin 43.

Key words: gap junction proteins, cell communication, morphogenesis, chick embryo, immunolocalization, nasal placode, primary palate, brain, retina.

Introduction

Mammalian embryonic facial development includes a sequence of events that results in the formation of outgrowths that enlarge and unite with each other to form the structures of the midface including the upper lip, nose and maxilla. The primordia that form these structures are the medial and lateral nasal processes, which arise as outgrowths on either side of the invaginating nasal placode, and the maxillary process, which emerges from the cranial end of the first pharyngeal arch. The fourth major primordium, the mandibular process, also arises from the first pharyngeal arch and forms the mandible, lower lip and associated structures (Streeter, 1948; Patten, 1968; Hamilton and Mossman, 1972; for avian development see Romanoff, 1960).

One of our major interests for the past several years has been the analysis of tissue interaction and spatial organization that result in the formation of these primordia, employing the chick embryo as a model system (Saber *et al.* 1989; Xu *et al.* 1990; Minkoff, 1990). Prior studies focused on the analysis of morphogenetic movement and cell cycle kinetics of facial mesenchyme (Minkoff and Kuntz, 1977, 1978; Minkoff, 1980*b*, 1984; Minkoff and Martin, 1984; Patterson *et al.* 1984; Patterson and Minkoff, 1985; Bailey *et al.* 1988). More recent studies of epithelial–mesenchymal interaction in the facial primordia (Saber *et al.* 1989; Minkoff, 1990) indicated the presence of stage-dependent gradients of cell viability of mesenchyme in organ culture. Developmental compartments, most noticeable at early stages of development, appeared within facial mesenchyme as a result of epithelial–mesenchymal interaction. The means by which these gradients and compartments could have been established led to a consideration of cell communication and signaling mechanisms.

Among the mechanisms by which cells communicate with each other during development, a region of junctional specialization in the plasma membrane – the gap junction – allows movement of water-soluble molecules having a molecular weight of less than

approximately 1000 to pass freely from the cytoplasm of one cell to another. A population of cells coupled by gap junctions becomes, therefore, a syncytium with regard to passage of ions and small molecules. This integrative effect can result in coordinate metabolic activity and could influence the activities of cell populations during inductive tissue interactions, morphogenetic change and pattern specification. Since gap junctions mediate ionic and metabolic coupling, the distribution of these membrane specializations would indicate the potential for metabolic coupling within specific anatomical regions or among particular cell populations.

In earlier studies, we had mapped the distribution of gap junctions in the facial primordia employing transmission electron microscopy (TEM). These analyses contained inherent limitations since large numbers of sections were required and only small areas could be studied at any given time. Therefore, indirect immunofluorescence employing antibodies to gap junction proteins (Hertzberg, 1984; Hertzberg and Skibbens, 1984; Hertzberg *et al.* 1985; Yamamoto *et al.* 1990) was utilized for localization. This provided a significant advantage since the distribution of gap junctions could be seen over large areas and allowed observations to be made that would not have been possible employing TEM or other related techniques.

Our studies utilized antibodies to connexin 32, a gap junction protein in rodent liver with an apparent mobility of approximately 27×10^3 M_r on SDS–PAGE (Henderson *et al.* 1979; Hertzberg and Gilula, 1979; Hertzberg, 1984; Paul, 1986). Immunocytological localization indicated that gap junctions were ubiquitously distributed throughout the epithelium and mesenchyme of all of the facial primordia examined. The distribution appeared uniform except in the developing nasal placode. In this structure, two sharply delineated regions were found. The superficial region contained a concentration of signal not found anywhere in the facial primordia or developing primary palate. Beneath this layer, the remaining deeper region of the placode was completely devoid of signal. This unusual pattern of distribution of gap junctions has been observed, thus far, in only one other tissue – the developing neuroepithelium.

Antibodies to connexin 43 (Beyer *et al.* 1987; Beyer *et al.* 1988), a gap junction protein initially isolated from heart tissue (Manjunath and Page, 1985), were also utilized as part of our ongoing efforts to map the distribution of gap junctions in developing chick facial primordia and nervous tissue. As in the case of connexin 32, a non-uniform distribution of immunoreactivity to connexin 43 was found, with an indication of only partial regional overlap of expression of these gap junction proteins.

Materials and methods

Tissue preparation

Fertile White Leghorn eggs were incubated at 37°C in a humidified atmosphere to yield normal embryos ranging between stages 22 and 28 (Hamburger and Hamilton, 1951; HH). This corresponds to 3 to 6 days of incubation and encompasses the formation of the primary palate in the chick embryo. Embryo heads were embedded in Tissue-Tek OCT compound (Miles Scientific, Naperville, IL) and rapidly frozen by immersion in liquid nitrogen. 10 μm cryostat sections were mounted on gelatinized slides. The slides were stored at −20°C until stained (refer to Fig. 1 for orientation and plane of sectioning).

Immunofluorescence

Tissue sections were incubated for 20 min with 10% rabbit serum in phosphate-buffered saline (R-PBS) to block non-specific binding of antibodies. After overnight incubation at 4°C with a 1:400 dilution of 2.0 μg ml^{-1} affinity-purified sheep antibodies to the 27×10^3 M_r rat liver gap junction protein in R-PBS, the slides were washed in PBS and incubated for one hour at room temperature with a 1:60 dilution in R-PBS of pre-adsorbed fluorescein-conjugated rabbit anti-sheep IgG (ICN, Lisle, IL). The fluoresceinated IgG was pre-adsorbed for 1 h at room temperature with a homogenate of chick embryo tissue, centrifuged and the supernatant fraction pre-adsorbed a second time. Serum was substituted for gap junction antibody in negative control slides. The slides were washed and mounted with glycerol containing 10% PBS and 1% p-phenylenediamine (PPD) to reduce photo-bleaching (Johnson and de C. Nogueira Araujo, 1981). In preliminary experiments, a high background due to the fluorescein-conjugated anti-sheep IgG secondary antibody was found with a sparse, but reproducible, signal discernible. The absorption protocol described above was, therefore, developed to lower this background. However, even with this approach and with the use of PPD, a labile signal was observed which was subject to relatively rapid photo-bleaching.

Rabbit antibodies to a peptide corresponding to amino acids 346–360 of the 43×10^3 M_r 'heart' sequence (Beyer *et al.* 1987) were employed in a similar fashion (Yamamoto *et al.* 1990). Tissue sections were blocked with 3% bovine albumin in PBS (BSA/PBS). After overnight incubation with a 1:1000 dilution of the primary antibody in BSA/PBS, slides were washed in PBS and incubated for one hour at room temperature with a 1:60 dilution of fluorescein-conjugated goat anti-rabbit IgG (Sigma). Slides were washed and mounted as described above.

Specimens were then examined with a Nikon Optiphot microscope equipped for epifluorescence. Photographs were prepared using Tri-X Pan ASA 400 film. The number of sections examined by developmental stage is displayed in Table 1.

Western blot analysis

Affinity-purified sheep antibodies to connexin 32 (Hertzberg, 1984; Saez *et al.* 1990) and a rabbit antibody to connexin 43 (Yamamoto *et al.* 1990) were used to identify immunoreactive proteins on Western blots. Tissue samples for Western blots were homogenized in 1 mM $NaHCO_3$ to which phenylmethylsulfonyl fluoride was added to 2 mM immediately before use from a 0.1 M stock solution in isopropanol. 50 μg protein samples were resolved by electrophoresis on 10% SDS–polyacrylamide gels, electrophoretically transferred to nitrocellulose and placed in a block solution overnight prior to incubation with primary antibodies (Hertzberg and Skibbens, 1984; Hertzberg *et al.* 1988). Subsequent to incubation with primary antibody, blots probed with sheep antibody were incubated with rabbit anti-sheep IgG followed by ^{125}I-Protein A. Blots probed with rabbit antisera were incubated with ^{125}I-

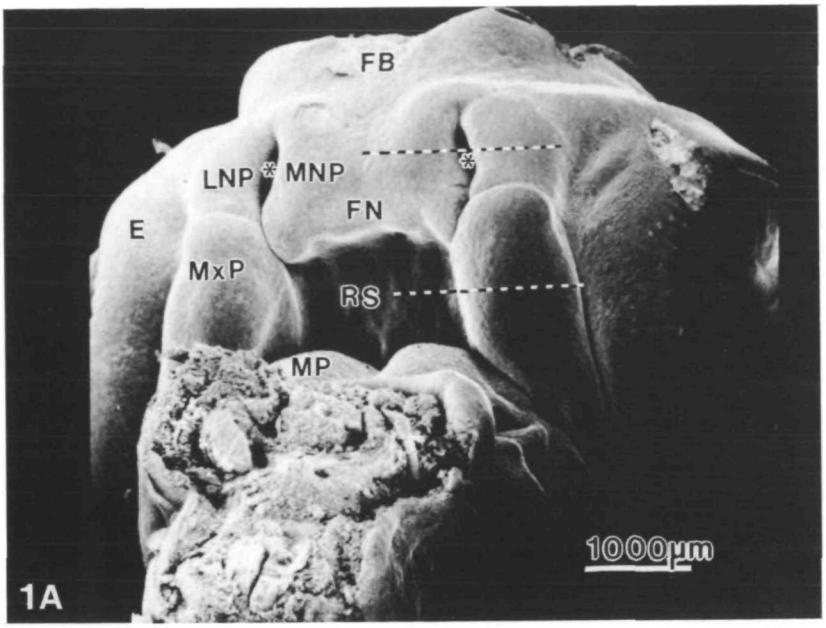

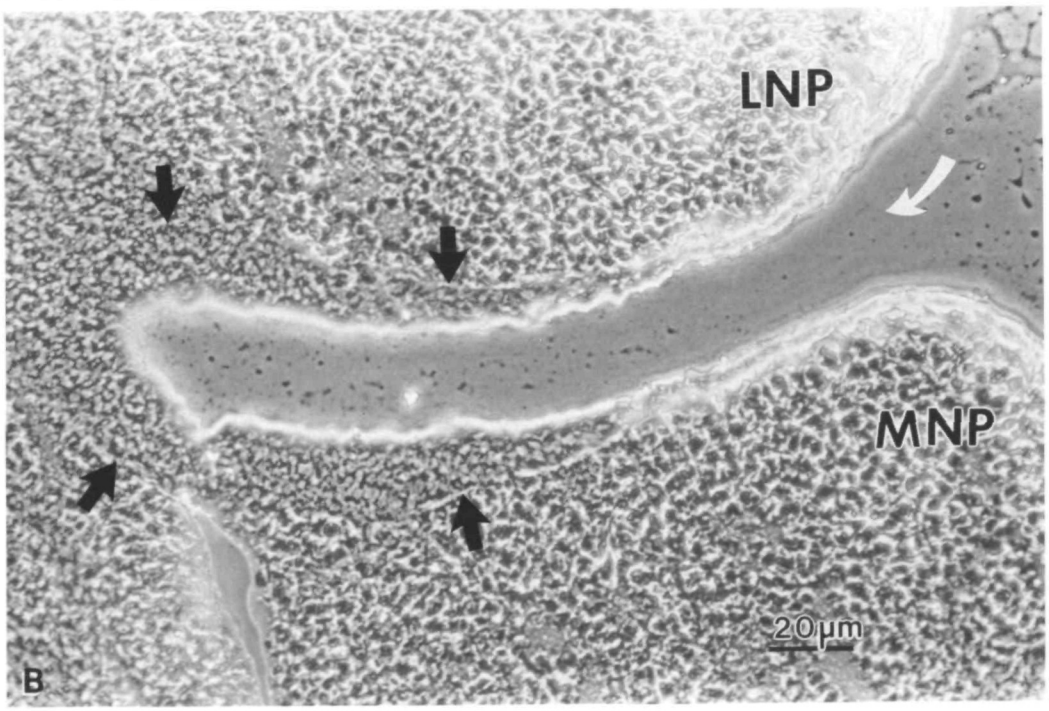

Fig. 1. (A) Scanning electron microscopic photograph of a chick embryo (approximately 5 days) illustrating the facial primordia and adjacent regions including the maxillary process (MxP), mandibular process (MP), lateral nasal process (LNP), medial nasal process (MNP), roof of the stomodeum (RS) and frontonasal region (FN). The invaginated nasal placodes are indicated by stars (*). The eye (E) and forebrain (FB) are also identified. Dotted lines indicate planes of sectioning in the maxillary and nasal processes. Photograph courtesy of Dr K. K. Sulik. (B) Phase-contrast tissue section through the nasal placode illustrating the relationships shown above in (A). Black arrows delineate the outline of the invaginated nasal placode. White arrow indicates orifice of the nasal groove.

Table 1. *Number of sections examined (from approximately 50 embryos)*

Embryo stage	Sections
22	225
25	483
28	240
	Total: 948

Protein A directly, and all autoradiographs exposed at −80°C using an intensifying screen. For samples in which preliminary experiments indicated an absence or low level of immunoreactivity, membrane protein-containing fractions enriched for gap junction proteins were prepared by extracting the homogenate in 20 mM NaOH and analyzing the material in the pellet obtained by centrifugation at 48000 *g* for 20 min (Hertzberg and Skibbens, 1984).

Antibody characterization

The localization of connexin 32-containing gap junctions was accomplished employing indirect immunofluorescence localization with antibodies raised against the 27×10^3 M_r rat liver gap junction protein. Based upon double diffusion analysis in which precipitin arcs were observed, the antibodies were directed against multiple determinants on the junction polypeptide. Specificity for the 27×10^3 M_r gap junction polypeptide has been demonstrated by immunoreplica analysis of liver plasma membranes and isolated gap junctions. By indirect immunofluorescence staining, the antibodies appear to bind to punctate regions of the hepatocyte plasma

membrane in a manner consistent with the distribution of gap junctions determined by electron microscopy (Hertzberg, 1984, 1985). Cross-reacting $27\times10^3 M_r$ polypeptides were detected in liver from mammalian, fish and avian species, including chick, by immunoreplica analyses and were localized to punctate regions of the plasma membrane by indirect immunofluorescence (Hertzberg and Skibbens, 1984; Dermietzel *et al.* 1984). Polyclonal antibodies to peptides in the $43\times10^3 M_r$ 'heart' gap junction protein (peptide 346–360 of the heart sequence conjugated to BSA) were also employed for Western blot analysis and immunolocalization (Yamamoto *et al.* 1990).

Transmission electron microscopy

Nasal placodes were dissected from stage 25 chick embryos and immediately placed in 3% buffered glutaraldehyde at 4°C for 24 h.

The tissues were rinsed in cold Millonig's phosphate buffer at pH 7.4 and post-fixed in 2% phosphate-buffered osmium tetroxide for 60 min at 4°C. The tissue was then rinsed with Millonig's phosphate buffer and dehydrated with three successive changes of ethanol for 15 min at each ethanol concentration (50%-70%-95%-100%), 3 changes of propylene oxide, and a final change of 1 part propylene oxide to 1 part epoxy resin uncorked overnight on a rotator. The supernatant fraction was decanted and the tissue was infiltrated with epoxy resin in a tightly corked vial for 1 h on a rotator and then transferred to capsules with epoxy mixture and allowed to polymerize overnight at 65°C. Thin sections were prepared and viewed on a JEOL-JEM-100CXII electron microscope.

Results

Immunofluorescent localization employing antibodies to the $27\times10^3 M_r$ gap junction protein revealed a ubiquitous distribution of immunoreactivity in both the mesenchyme and epithelium in all of the facial primordia as well as adjacent regions such as the roof of the stomodeum at all stages examined. Distinct punctate signal was seen throughout the mesenchyme and epithelium. There was a uniform distribution of signal with no indication of concentration in specific regions. This uniform and ubiquitous distribution can be seen in representative sections from the maxillary and lateral nasal processes and roof of the stomodeum at stage 22 (Fig. 2), the medial nasal and mandibular processes and roof of the stomodeum at stage 25 (Fig. 3), and from the maxillary process and frontonasal region at stage 28 (Fig. 4). TEM photographs (Fig. 5) confirmed the presence of gap junctions in both epithelium and mesenchyme. In a prior TEM study, gap junctions were found throughout mesenchyme not only between cell bodies but between cell bodies and cell processes and between cell processes (unpublished data).

The only exception to this ubiquitous distribution of gap junctions was a unique non-random pattern found in the epithelium of the nasal placode (Fig. 6). In this region, a distribution characterized by two zones was found; a distinct heavy concentration of signal in the superficial layer of cells adjacent to the exterior surface and a region devoid of detectable signal in the interior cell layer of the nasal placode adjacent to the mesenchyme. This pattern was seen during all stages of placode invagination that were examined. For example, in Fig. 6A this distinctive pattern is seen at the base of the nasal placode at stage 22 where signal is found only in the region adjacent to the nasal groove. The deeper cell layers of placodal epithelium are completely devoid of signal. In contrast, the subjacent mesenchyme displays the characteristic uniform distribution of signal found throughout the primordia of the developing face. The corresponding pattern was seen in nasal placode epithelium at stages 25 (Fig. 6B) and 28 (Fig. 6C).

A distinct change in the distribution of signal could be seen in the region where the placodal epithelium merges with the epithelium of the medial and lateral nasal processes (Fig. 7). In this transitional zone, the uniform distribution of signal in the epithelium of the nasal primordia becomes restricted to the superficial layers of the epithelium; in the thickened, invaginated region of the placode, the characteristic two zones are seen.

This pattern of distribution of signal was also observed in developing neuroepithelium of the brain (Fig. 8A and B). Here, as in the nasal placode, two zones were delineated. An extremely heavy concentration of signal was found in the neural epithelium lining the ventricles of the brain. The deeper layers were devoid of signal and presented a pattern identical to that of the placodal epithelium (compare Fig. 8 with Fig. 6 and 7). Separation of signal was also observed in the neural retina (Fig. 8C). In this instance, however, signal was concentrated in the layer adjacent to the pigmented retina. Because of the inversion of cell layers during optic cup formation, the region in which signal was concentrated in the neural retina corresponds to the cell layer lining the ventricle of the brain.

It should be noted that no physical barriers exist between the two regions in either the nasal placode or the brain. In the nasal placode the cells are contiguous with no morphological boundaries such as a basement membrane separating the cell layers (Fig. 9).

Preliminary studies employing immunolocalization with antibodies to connexin 43 also revealed non-random patterns of distribution. In contrast to the

Fig. 2–4. Representative immunofluorescence photomicrographs of frozen sections of facial primordia and adjacent structures stained with antibody to the $27\times10^3 M_r$ gap junction protein as described in Materials and methods. Fig. 2. Stage 22 (approximately 3½–4 days of incubation). Tissue from the maxillary process (A), lateral nasal process (B) and roof of the stomodeum (C). Fig. 3. Stage 25 (approximately 5 days of incubation). Tissue from the medial nasal process (A), mandibular process (B) and roof of the stomodeum (C). Fig. 4. Stage 28 (approximately 6 days of incubation). Tissue from the maxillary process (A) and the frontonasal region (B). A negative control section through the medial nasal process (Stage 25) in which primary antibody was omitted is shown in Fig. 4C. Note the ubiquitous distribution of punctate signal throughout the mesenchyme and epithelium in all of the regions examined. Epi, epithelium; Mes, mesenchyme. Magnification for Figs 2, 3 and 4 is shown in Fig. 2B.

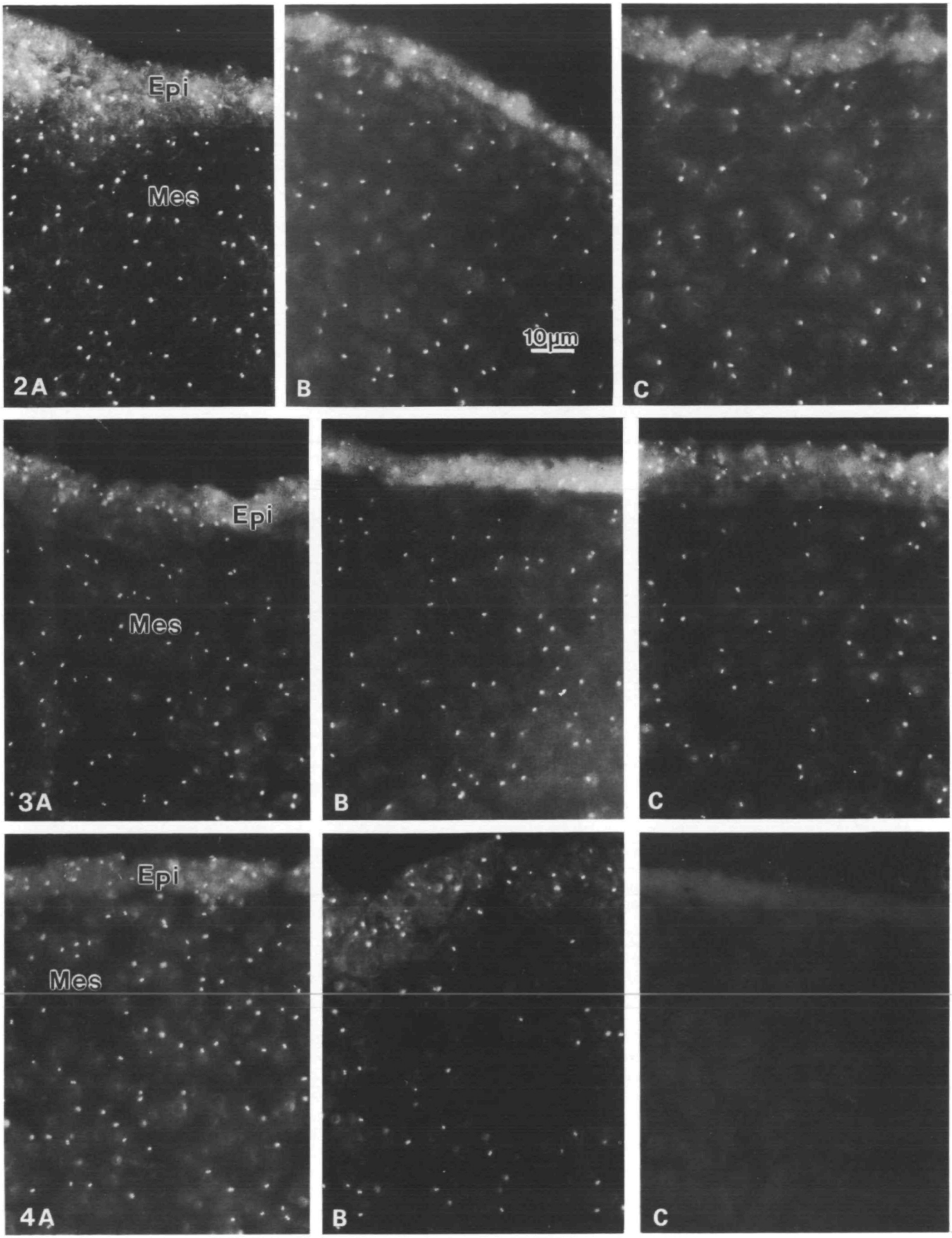
Epi
Mes
2A
B
10μm
C
Epi
Mes
3A
B
C
Epi
Mes
4A
B
C

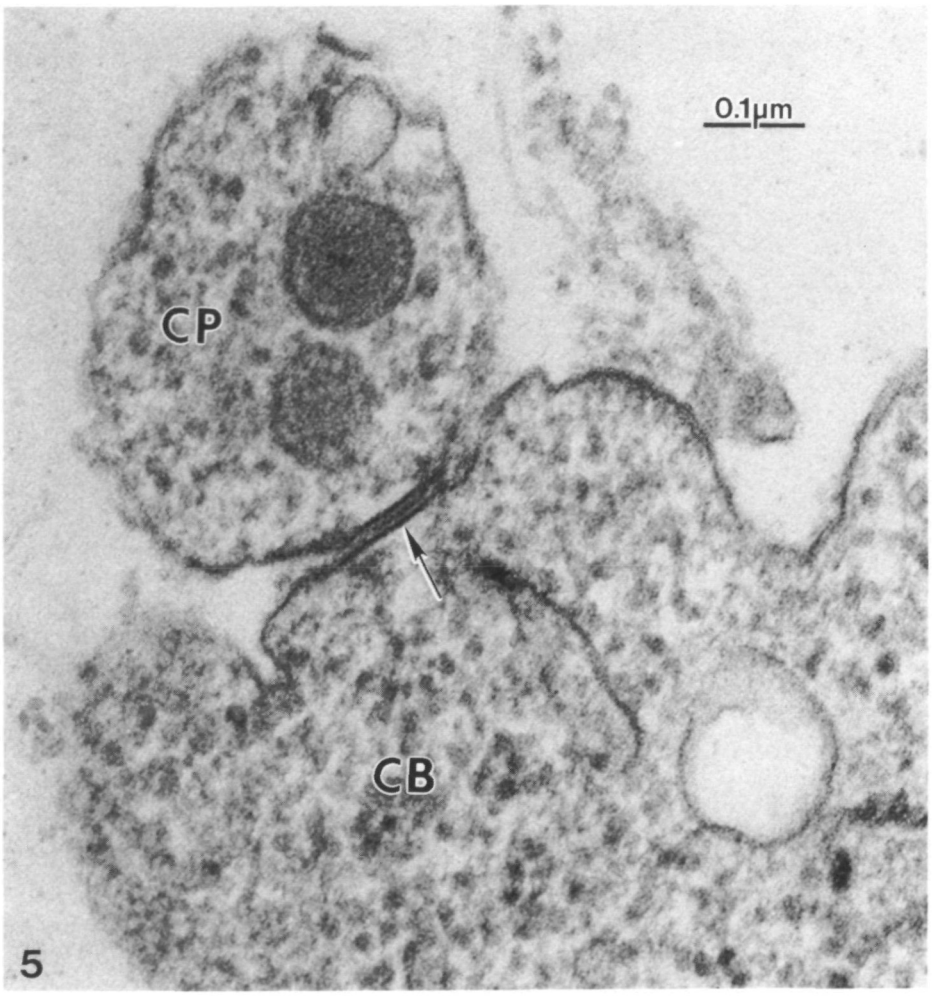

Fig. 5. Transmission electron microscope (TEM) photograph of a representative gap junction (arrow), located between a cell body (CB) and a cell process (CP), typical of those found in embryonic facial mesenchyme.

relatively photo-labile signal obtained with the anti-connexin 32 antibodies, a robust, stable signal was obtained with our antibodies to connexin 43. Initial studies with these antibodies indicate concentration of signal in the cell layers of the brain adjacent to the ventricle (Fig. 10). Distinct patterns of distribution also appear to be present in the retina. These patterns, in both the brain and retina, however, are somewhat discordant from those found with antibodies to the $27\times10^3 M_r$ protein (compare Fig. 10 with Fig. 8). In addition, initial observations of distribution patterns in mesenchyme with antibodies to the $43\times10^3 M_r$ protein indicate regional concentrations of signal, most noticeably in the lateral and medial nasal processes (data not shown). These patterns appear markedly different from those found with antibodies to the $27\times10^3 M_r$ protein.

Identification of immunoreactive proteins recognized by these antibodies immunocytologically (above) was undertaken by Western blot analysis (Fig. 11). Pooled brain, retina and placode homogenates were analyzed using the antibodies to connexin 32 (Fig. 11A) and connexin 43 (Fig. 11B).

In most experiments with antibodies to connexin 32, it was difficult to resolve, reproducibly, antibody binding to proteins in chick samples even when membrane proteins were concentrated by extraction of soluble and peripheral membrane proteins with alkali. In some experiments, however, antibody binding was observed to proteins in the alkali residue of the chick material which co-migrated with $27\times10^3 M_r$ liver gap junction protein and its $47\times10^3 M_r$ dimer (Fig. 11A). Unlike the situation with the anti-connexin 32 antibodies, protein in the chick homogenate co-migrating with heart connexin 43 was generally detectable (not shown), as it was in alkali-residues (Fig. 11B). The difference between detectability of connexin 43 and connexin 32 immunoreactivity on Western blots appears to correlate with the difficulties encountered in obtaining clear, but labile, signal immunocytologically

Fig. 6. Immunofluorescence photomicrographs of frozen sections through the base of the nasal placode (region of deepest invagination) from chick embryos of stages 22 (A), 25 (B) and 28 (C) stained with antibody to the $27\times10^3 M_r$ gap junction protein. Note the heavy concentration of signal in the superficial cell layers close to the surface of the placode and the absence of signal in the deeper layers of the placode adjacent to the mesenchyme. (D) Negative control of stage 28 placode in which primary antibody was omitted. PE, placodal epithelium; Mes, mesenchyme. Stars (*) indicate lumen of nasal groove. Arrows delineate outline of nasal placodes. Magnification of A–D is shown in B.

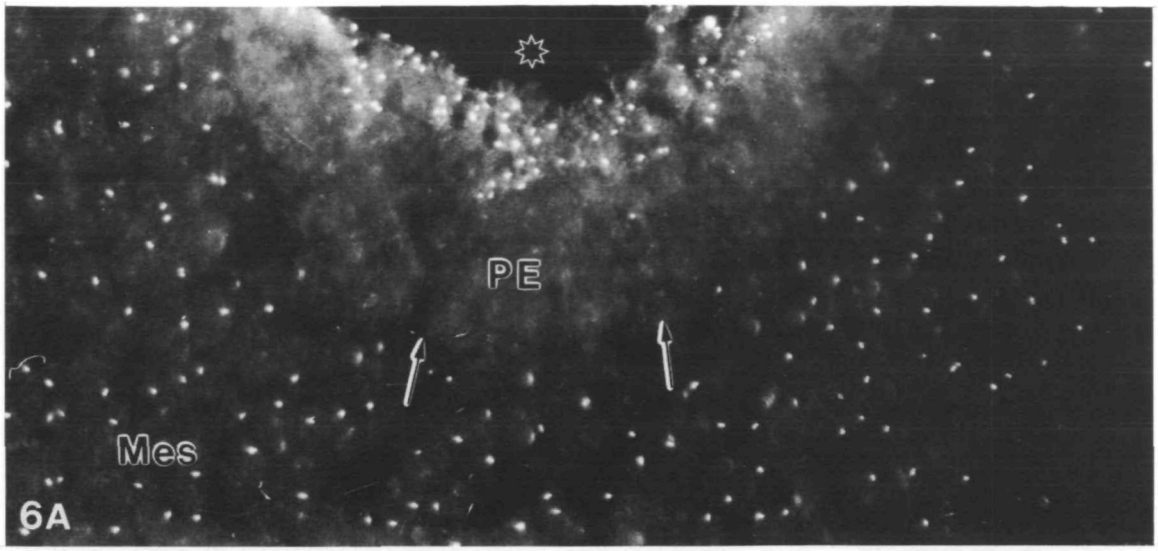
PE
Mes
6A

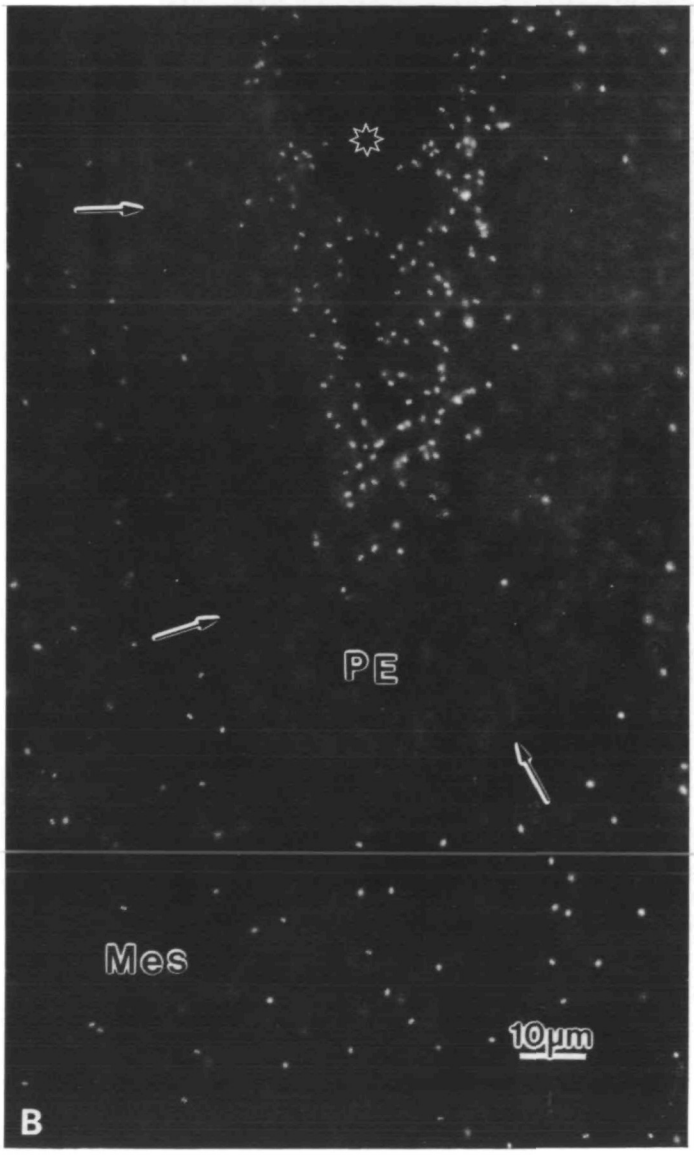
PE
Mes
10μm
B

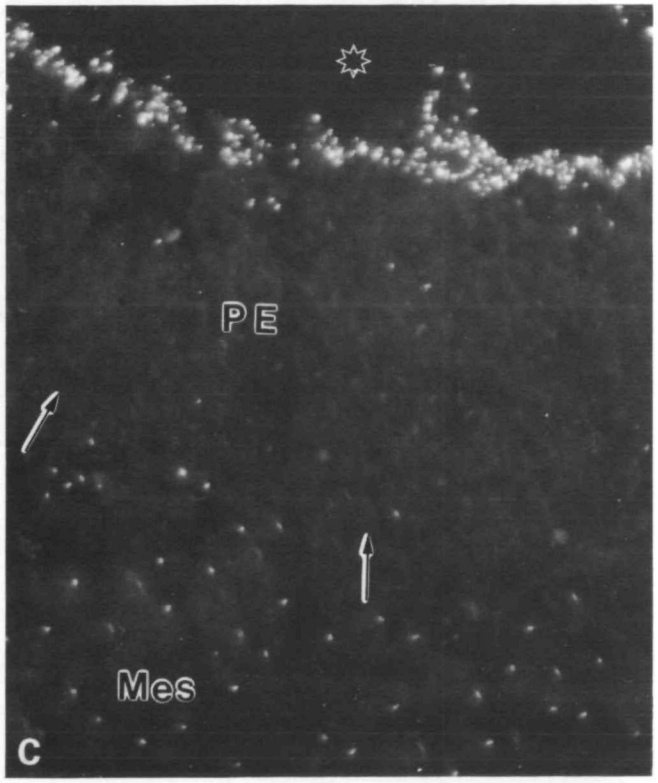
PE
Mes
C

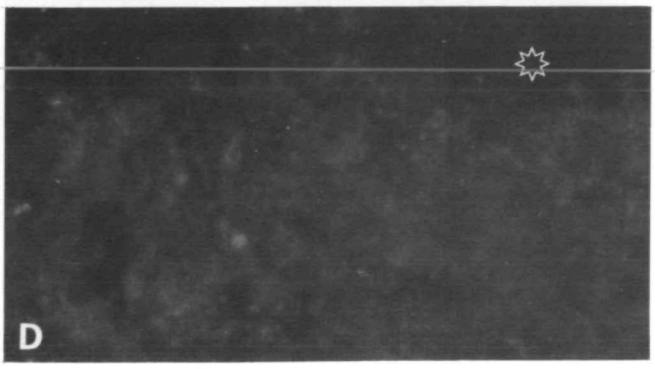
D

with the connexin 32 antibody and is likely to reflect the relative abundance of these proteins in the samples analyzed. However, it is also possible that tissue manipulations prior to SDS–PAGE lead to differences in recovery of these connexins. Alternatively, greater differences may exist in the primary structure of chick

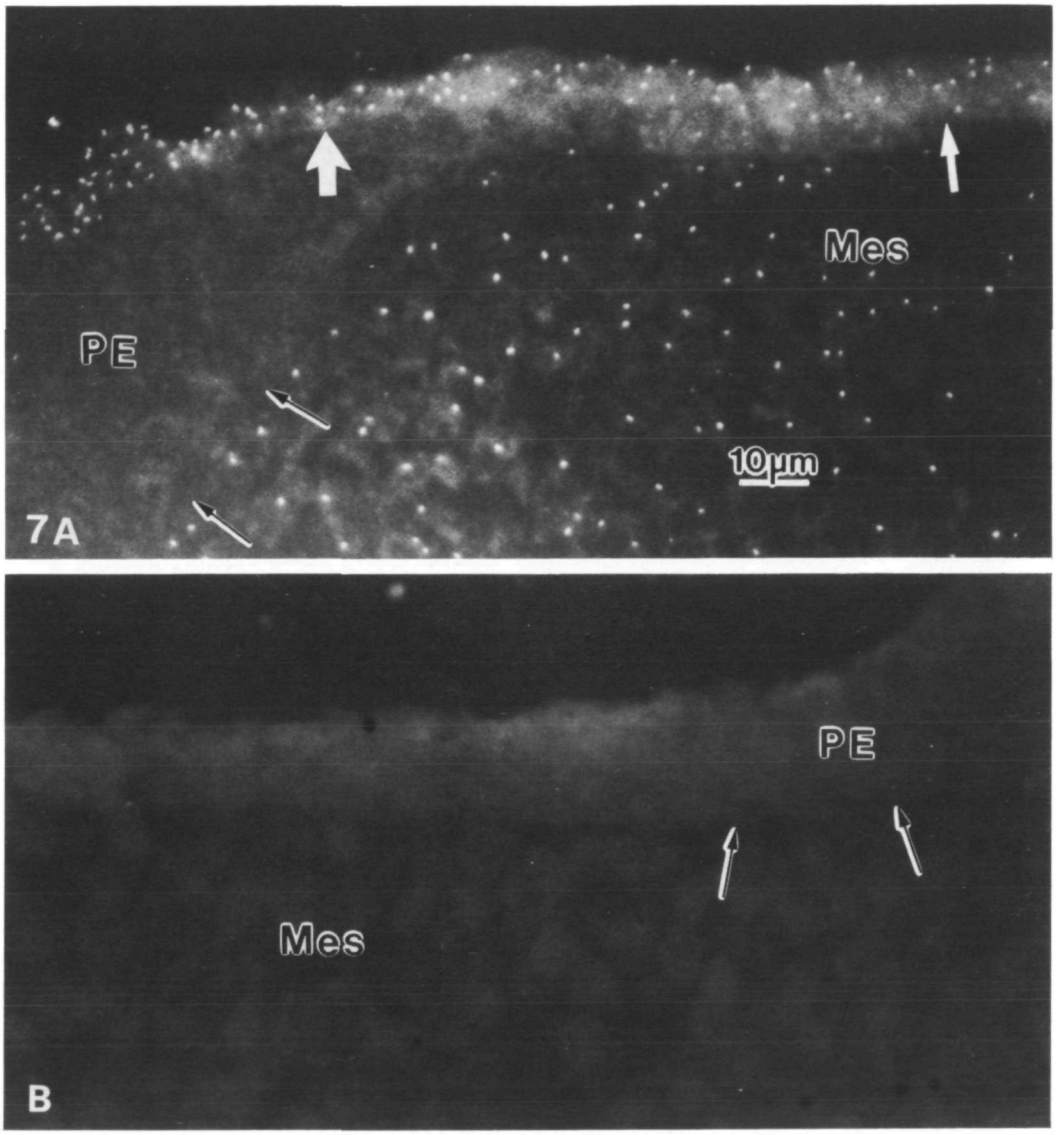

Fig. 7. Immunofluorescence photomicrograph of a frozen section of a stage 25 embryo stained with antibody to the 27×10^3 M_r gap junction protein, through the boundary of the nasal placode where the placodal epithelium merges with the epithelium of the medial and lateral nasal processes. Note the transition from a uniform distribution of signal found in the epithelium of the nasal primordium (thin white arrow) with the concentration of signal in the surface cell layer of the placodal epithelium (thick white arrow). The deeper layer of placodal epithelium (PE) is devoid of signal. Compare Fig. 7 with Figs 2B and 3A. A negative control section through the transitional region of the nasal placode is shown in Fig. 7B. Black arrows delineate outlines of nasal placodes in A and B. Mes, mesenchyme. Magnification of A and B is shown in A.

Fig. 8. Immunofluorescence photomicrographs of frozen sections through the developing central nervous system of chick embryos at stages 22 (A) and 25 (B), stained with antibody to the 27×10^3 M_r gap junction protein. Note the concentration of signal on the surface of the neural epithelium lining the ventricles (thick white arrows) and the absence of signal in the deeper regions demonstrating a pattern identical to that found in the nasal placode (compare with Figs 6 and 7). NE, neural epithelium. Frozen sections through the retina (C) stained with antibody to the 27×10^3 M_r gap junction protein show concentration of signal in the neural retina (NR), in the cell layers adjacent to the pigmented retina (PR). The adjacent cell layers in the NR are devoid of signal. The space between the PR and NR is an artifact of sectioning. (D,E) Negative controls of (A) and (B) respectively in which primary antibody was omitted. White arrows indicate the surface of the neural epithelium. Magnification of (A–E) is shown in (B). Mes, mesenchyme.

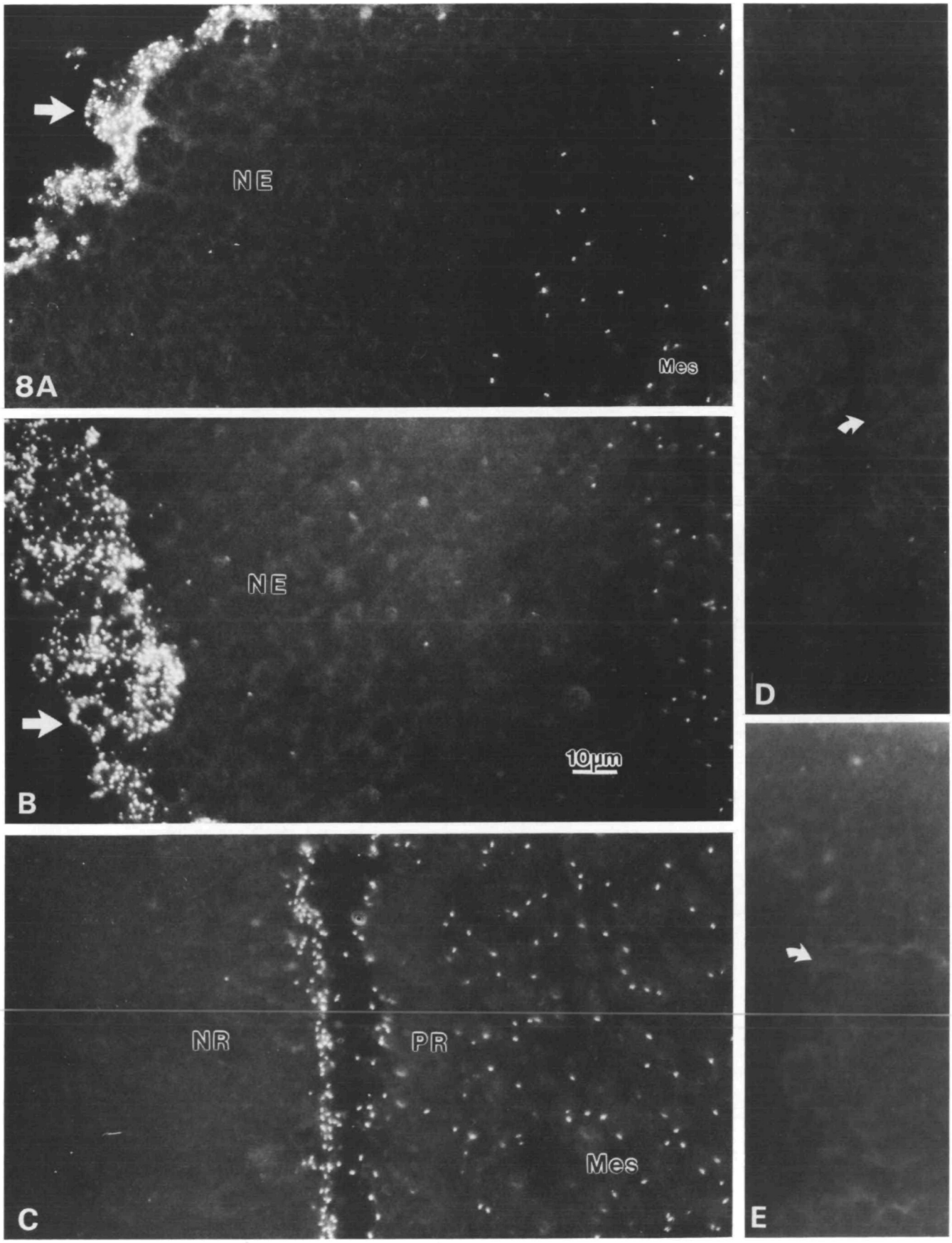
NE
Mes
8A
NE
10μm
B
D
NR
PR
Mes
C
E

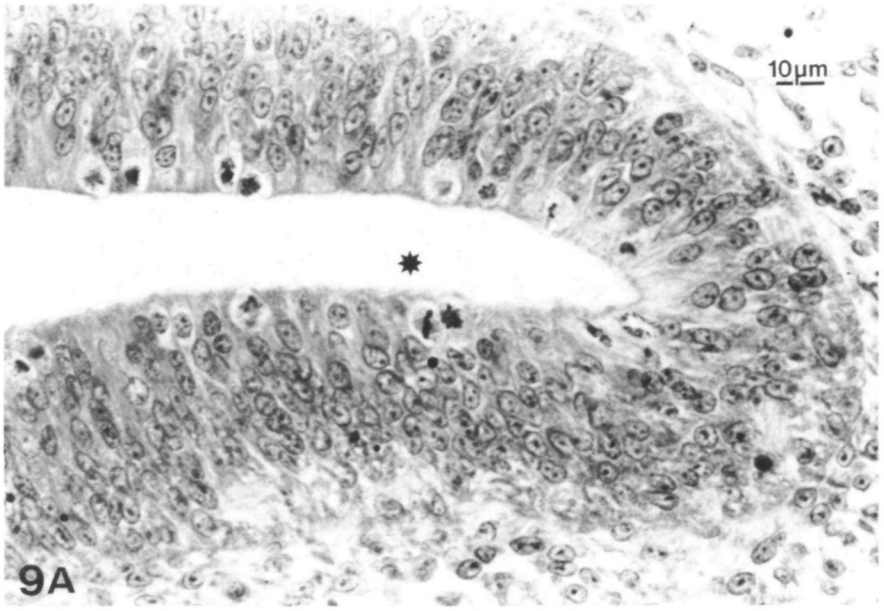

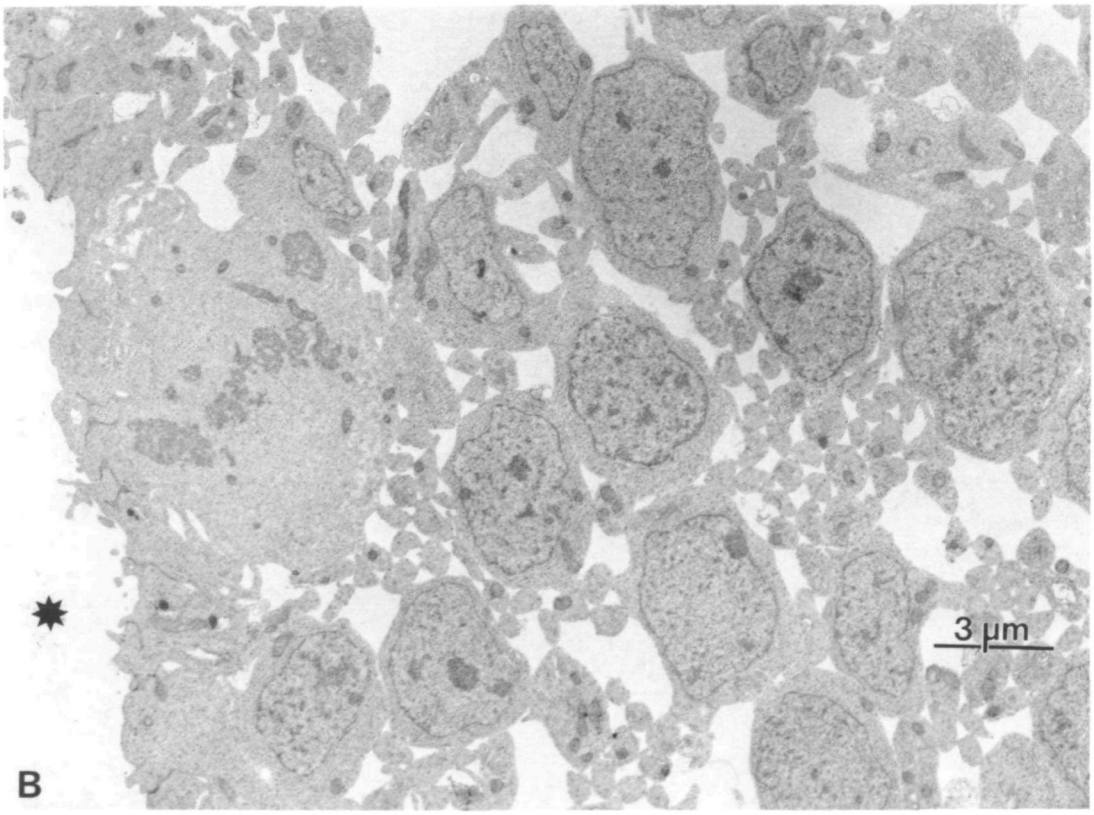

Fig. 9. Bright-field photomicrograph (A) of a section through the nasal placode stained with hematoxylin and eosin. (B) A TEM photograph of a corresponding region of the nasal placode adjacent to the lumen of the nasal groove (star). No morphological boundaries are apparent between the superficial and deeper cell layers of the placodal epithelium.

connexin 32 relative to that of rat as compared to the sequence of connexin 43 containing the peptide to which the anti-connexin 43 antibody was raised.

Discussion

Localization of structures immunoreactive with an antibody to the 27×10^3 M_r liver gap junction protein (Hertzberg, 1984; Hertzberg and Skibbens, 1984), also referred to as connexin 32 (Paul, 1986) has revealed a ubiquitous distribution of immunoreactivity in all regions of the primary palate including the facial primordia. The distribution appeared to be uniform without region-specific concentration of signal in either mesenchyme or epithelium with the exception of one structure – the nasal placode. In the placodal epithelium, a unique, non-random pattern of distribution of signal was found.

The uniqueness of this pattern was striking. In only one other region of the craniofacial complex was such a pattern observed. The developing neuroepithelium of the brain and retina displayed compartmentalization of

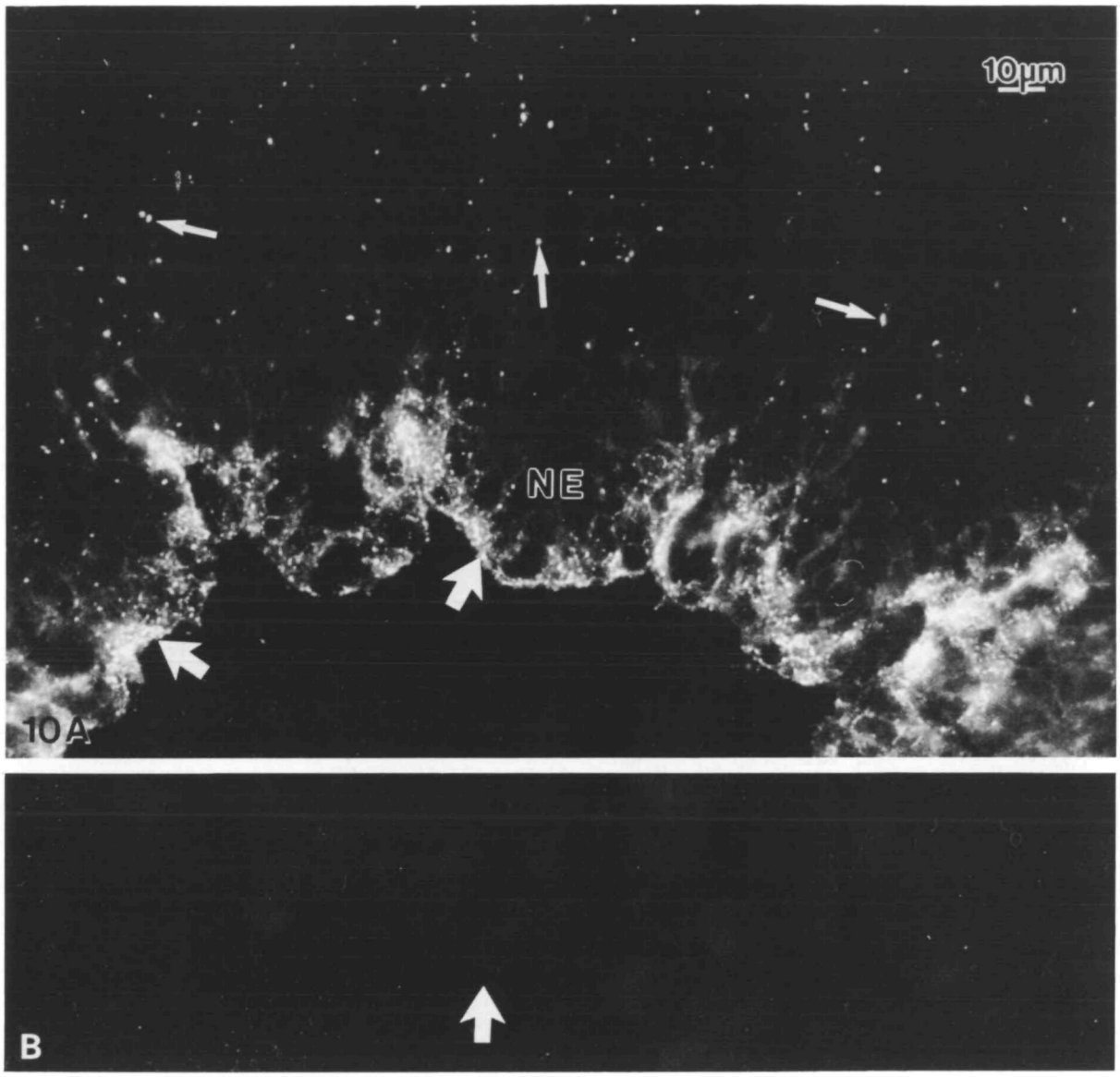

Fig. 10. Immunofluorescence photomicrographs of frozen sections through the developing brain of a stage 28 chick embryo (A) stained with antibody to the 43×10^3 M_r gap junction protein. Note the concentration of signal on the surface of the neuroepithelium lining the ventricles (thick white arrow). In contrast to the neuroepithelium of the same and earlier stages stained with antibody to the 27×10^3 M_r protein, the deeper layers of the brain appear to contain uniformly distributed and diffuse signal (thin white arrows). (B) Negative control in which primary antibody was omitted. White arrow indicates the surface of the neural epithelium. Magnification of (B) is shown in (A). N.E., neural epithelium.

signal. For example, neuroepithelium lining the ventricles of the brain contained a concentration of signal as dense as that found in the superficial layers of the placodal epithelium. In a similar fashion, the deeper layers of the neuroepithelium were devoid of signal. It is noteworthy that prior studies, employing freeze fracture analysis (e.g. Revel and Brown, 1976; Schoenwolf and Kelley, 1980), suggested the presence of juxtaluminal concentrations of gap junctions during development of the neural tube in the chick embryo. More recently Dermietzel *et al.* (1989) demonstrated the presence and regional distribution of gap junction proteins (connexin 26 and 43) in the developing mammalian brain. A pattern of immunoreactivity was observed that revealed separation of signal between the ventricular and subventricular zones similar in appearance to what was observed in the present study of the embryonic avian brain.

The reasons for the presence of this unique pattern are, at present, obscure. In both instances, the cell layers containing dense concentration of signal are zones of cell proliferation where all mitotic activity within the epithelium occurs. Communication by means of gap junctions could serve to synchronize those cell populations for co-ordinate proliferative activity. This, however, does not explain why the deeper regions of the cell layers of either structure are devoid of signal although it is possible that a different protein, not

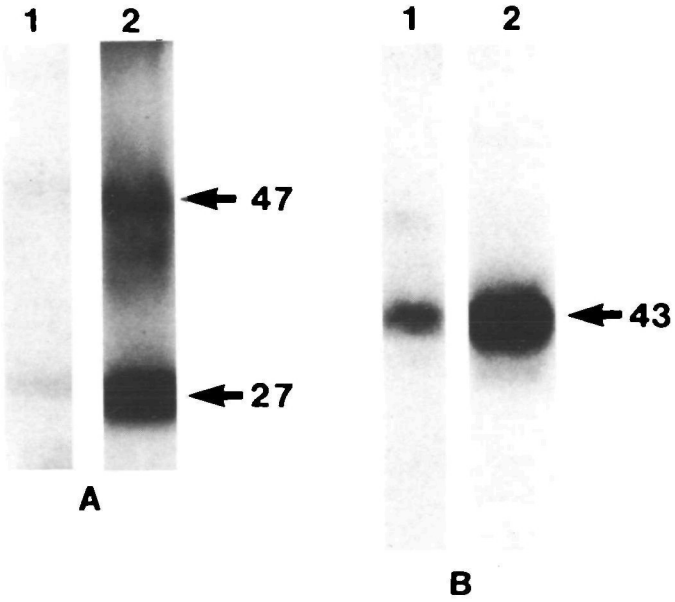

Fig. 11. Connexin identification in pooled chick brain, retina and nasal placode. Pooled tissue from brain, retina and nasal placode were analyzed as base-treated residues by Western blots. Samples in blot 'A' compared base-treated pooled stage 28 chick tissue residue (lane 1) with similarly prepared rat liver material (lane 2). Samples in blot 'B' compared pooled stage 28 chick tissue base-treated residue (lane 1) with a crude rat heart homogenate (lane 2). Blot 'A' was treated with affinity-purified anti-connexin 32 antibody and blot 'B' was treated with polyclonal antiserum to a connexin 43 peptide corresponding to amino acids 346–360 of the connexin 43 sequence. In 'A' the positions of the 27×10^3 M_r connexin 32 monomer and its 47×10^3 M_r dimer are indicated. In 'B' the position of the heart connexin 43 protein is indicated. The faster migrating proteins in this sample correspond to dephosphorylated forms of the protein (Hertzberg *et al.* submitted for publication).

recognized by our antibodies, is expressed in gap junctions of these regions. In the case of the developing brain, the deeper layer – the mantle layer – contains differentiating neurons that may require the absence of cell communication by means of gap junctions as part of the program by which axonal specificity is established. In this regard, it should be noted that in regions such as the developing retina of the chick embryo, associations have been found between the disappearance of gap junctions and the progressive differentiation of neural epithelium (Fujisawa *et al.* 1976).

This, however, would not be the case with placodal epithelium. Although olfactory neurons arise from the base of the nasal placode and send axonal projections to the olfactory centers of the brain, the major cell type in the nasorespiratory tract is pseudostratified ciliated columnar epithelium. In addition, other cell types are present whose lineage is, presumably, from placodal epithelium. It is difficult, therefore, to envision the necessity for an impedence of cell communication among cell populations with such diverse lineages.

Two recent studies that, however, may be of potential relevance to the pattern of distribution in placodal epithelium concern the origin of neurons of the central nervous system that produce luteinizing hormone – releasing hormone (LHRH) and which control the release of gonadotropic hormones from the anterior pituitary. These reports (Schwantzel-Fukuda and Pfaff, 1989; Wray *et al.* 1989) provide evidence that these cells originate in the olfactory epithelium and migrate into, and then through, the forebrain. Their path of migration is associated with the nervus terminalis medial to the axons of the olfactory nerves (Schwantzel-Fukuda *et al.* 1989). Many of the immuno-positive-stained LHRH cells that migrated out of the olfactory epithelium formed what were described as 'tracks'. These cells differed morphologically from those within the olfactory epithelium in that the former now became bipolar or unipolar and contained processes that appeared to contact each other (Wray *et al.* 1989). Since these 'tracks' extended from the olfactory epithelium into the telencephalon and rostral diencephalon, it is not unreasonable to consider a role for gap junctions in the coordination of migratory activity of this unique cell population.

An alternative explanation for the presence of this unusual pattern of gap junction distribution, and, by implication, of cell communication, may be related to morphogenetic changes that occur in these structures. The nasal placode invaginates to form a pit, then a groove and finally a tube, forming the nasal chamber and associated structures. The developing brain also undergoes numerous alterations in form associated with flexure of the neural tube, enlargement of hemispheres, constrictions, etc. The uniqueness of the pattern of gap junction distribution could be associated with the coordination of cell movement required for these extensive morphological changes that accompany the development of these structures.

In a prior study, performed several years ago (Minkoff, 1983), the distribution of gap junctions in mesenchyme of the maxillary process and the roof of the stomodeum was mapped employing transmission electron microscopy. A non-random distribution was found in this preliminary study which indicated that the concentration of gap junctions was greater in mesenchyme subjacent to maxillary process epithelium. Further, it was observed that the distribution of gap junctions in these regions (i.e. the maxillary process and roof of the stomodeum) tended to parallel previously reported differences in rates of cell proliferation (Minkoff and Kuntz, 1978; Minkoff, 1980*a*). These differences in gap junction distribution, however, were not supported by analysis employing immunolocalization with antibody to the 27×10^3 M_r gap junction protein. The latter analysis demonstrated a random distribution in the mesenchyme of both the maxillary process and roof of the stomodeum.

These contradictions may be a reflection of the necessity to examine very small regions of the maxillary process and roof of the stomodeum with TEM and then to combine these data for analysis. The difficulties encountered in obtaining greater amounts of data and

increased sample size led to the use of alternative techniques employed in the present study. Quantitative analysis of the numbers of gap junctions and cell bodies per unit area, however, employing immunofluorescent localization with antibodies to the $27\times10^3 M_r$ protein indicated a random distribution even when normalized for cell number (data not shown). The resolution of this issue will require additional studies, now in progress, with antibodies to other gap junction proteins. Preliminary studies of $43\times10^3 M_r$ gap junction distribution, as noted above, revealed concentrations of signal in the nasal primordia and show promise of clarifying this issue.

The pattern of immunoreactivity described for the $27\times10^3 M_r$ protein may well represent but a subset of gap junctions recognized by these antibodies. Distinct proteins homologous to the $27\times10^3 M_r$ liver gap junction protein (Beyer *et al.* 1988) have been identified in liver ($21\times10^3 M_r$ on SDS–polyacrylamide gels) (Nicholson *et al.* 1987; Hertzberg *et al.* 1988), heart (connexin 43) (Manjunath *et al.* 1987; Beyer *et al.* 1987) and lens epithelial cells (MP70) (Kistler *et al.* 1988). It has also been shown that individual gap junctions can have more than one gap junction protein (e.g. 27 and $21\times10^3 M_r$ in hepatocytes (Nicholson *et al.* 1987)). Furthermore, heterologous coupling has been demonstrated in *Xenopus* oocytes expressing different connexin mRNAs leading to channels with asymmetric gating properties (Swenson *et al.* 1989; Werner *et al.* 1989). Hence, the possibility remains of communication compartments in the tissues examined beyond those delineated here. In addition, discrete regulatory mechanisms within regions of tissue reflecting gating properties of individual gap junction proteins (connexins) may also arise in these regions during development.

For these reasons, continuing studies of the $43\times10^3 M_r$ gap junction protein, as well as other gap junction proteins, are indicated especially in view of the difficulty encountered in obtaining a signal with antibodies to the $27\times10^3 M_r$ rat liver gap junction protein on Western blot analysis. Analysis of differential expression of gap junction proteins by Dermietzel *et al.* (1989) may be particularly significant in this regard. Connexins 26 and 43 were found in embryonic mammalian brain tissue while connexin 32 was reported to be virtually absent. Only after birth was connexin 32 expressed to a significant degree. This coincided with decreased expression of connexin 26 in the postnatal mammalian brain. Connexin 43 expression was observed in both embryonic and mature brain tissue. As noted by Dermietzel *et al.* (1989) discrepancies between this and other studies (Dudek *et al.* 1988; Nagy *et al.* 1988; Shiosaka *et al.* 1989) may be a result of differences in the composition of polyclonal sera.

The polyclonal antibody to the $27\times10^3 M_r$ gap junction protein employed in the studies reported here may have recognized a broader spectrum of antigenic sites, potentially including those on other connexins (or related proteins) present in an abundance too low to visualize routinely on Western blots. However, our ability to demonstrate antibody binding to a protein in chick samples co-migrating with liver connexin 32 in some, but not all, Western blot experiments does suggest its presence, albeit at low abundance, in these samples.

This study was supported by NIH grants DE-07674 (R.M.), GM30667 (E.L.H.) and a Research Career Development Award (HD00713 to E.L.H.). E.L.H. is the recipient of an Irma T. Hirschl Career Scientist Award. The authors wish to express their appreciation to Mr Udayan Parikh for assistance with the transmission electron microscopy, to Mr Richard Coprina for assistance with the Western Blots, and to Ms Barbara Barton for her expert secretarial assistance in the preparation of this manuscript.

References

Bailey, L., Minkoff, R. and Koch, W. E. (1988). Relative growth rates of maxillary mesenchyme in the chick embryo. *J. craniofac. gen dev. Biol.* **8**, 167–177.

Beyer, E. C., Goodenough, D. A. and Paul, D. L. (1988). The connexins, a family of related gap junction proteins. In *Gap Junctions*, (ed. E. L. Hertzberg and R. G. Johnson), pp. 167–175. New York: Alan R. Liss, Inc.

Beyer, E. C., Paul, D. L. and Goodenough, D. A. (1987). Connexin43: a protein from rat heart homologous to a gap junction protein from liver. *J. Cell Biol.* **105**, 2621–2629.

Dermietzel, R., Leibstein, A., Frixen, U., Janssen Timmen, U., Traub, O. and Willecke, K. (1984). Gap junctions in several tissues share antigenic determinants with liver gap junctions. *EMBO J.* **3**, 2261–2270.

Dermietzel, R., Traub, O., Hwang, T. K., Beyer, E., Bennett, M. V. L., Spray, D. C. and Willecke, K. (1989). Differential expression of three gap junction proteins in developing and mature brain tissues. *Proc. natn. Acad. Sci. U.S.A* **86**, 10148–10152.

Dudek, F. E., Gribkoff, V. K., Olson, J. E. and Hertzberg, E. L. (1988). Reduction of dye coupling in glial cultures by microinjection of antibodies against the liver gap junction polypetide. *Brain Res.* **439**, 275–280.

Fujisawa, H., Morioka, H., Watanabe, K. and Nakamura, H. (1976). A decay of gap junctions in association with cell differentiation of neural retina in chick embryonic development. *J. Cell Sci.* **22**, 585–596.

Hamburger, V. and Hamilton, H. L. (1951). A series of normal stages in the development of the chick embryo. *J. Morph.* **88**, 49–92.

Hamilton, W. J. and Mossman, H. W. (1972). *Human Embryology*. Baltimore: Williams and Wilkins.

Henderson, D., Eibl, H. and Weber, K. (1979). Structure and biochemistry of mouse hepatic gap junctions. *J. molec. Biol.* **132**, 193–218.

Hertzberg, E. L. (1984). A detergent-independent procedure for the isolation of gap junctions from rat liver. *J. biol. Chem.* **259**, 9936–9943.

Hertzberg, E. L. (1985). Antibody probes in the study of gap junctional communication. *A Rev. Physiol.* **47**, 305–318.

Hertzberg, E. L., Disher, R. M., Tiller, A. A., Zhou, Y. and Cook, R. G. (1988). Topology of the Mr 27,000 liver gap junction protein. Cytoplasmic localization of amino- and carboxyl termini and a hydrophilic domain which is protease-hypersensitive. *J. biol. Chem.* **263**, 19105–19111.

Hertzberg, E. L. and Gilula, N. B. (1979). Isolation and characterization of gap junctions from rat liver. *J. biol. Chem.* **254**, 2138–2147.

Hertzberg, E. L. and Skibbens, R. V. (1984). A protein homologous to the 27000 dalton liver gap junction protein is present in a wide variety of tissues and species. *Cell* **39**, 61–69.

Hertzberg, E. L., Spray, D. C. and Bennett, M. L. V. (1985). Reduction of gap junctional conductance by microinjection of antibodies against 27kD liver gap junctional polypeptide. *Proc. natn. Acad. Sci. U.S.A.* **82**, 2412–2416.

HERTZBERG, E. L., SPRAY, D. C. AND COOK, R. (1988). Biochemical, immunological and topological studies of gap junctions. In *Gap Junctions* (eds. E. L. Hertzberg and R. G. Johnson), pp. 9–28 New York: Alan R. Liss, Inc.

JOHNSON, G. D. AND DE C. NOGUEIRA ARAUJO, G. M. (1981). A simple method of reducing the fading of immunofluorescence during microscopy. *J. Imm. Methods* **43**, 349–350.

KISTLER, J., CHRISTIE, D. AND BULLIVANT, S. (1988). Homologies between gap junction proteins in lens, heart and liver. *Nature* **331**, 721–723.

MANJUNATH, C. K., NICHOLSON, B. J., TEPLOW, D., HOOD, L., PAGE, E. AND REVEL, J. P. (1987). The cardiac gap junction protein (Mr 47,000) has a tissue-specific cytoplasmic domain of Mr 17,000 at its carboxy-terminus. *Biochem. biophys. Res. Commun.* **142**, 228–234.

MANJUNATH, C. K. AND PAGE, E. (1985). Cell biology and protein composition of cardiac gap junctions. *Am. J. Physiol.* **248**, H783–H791.

MINKOFF, R. (1980*a*). Cell proliferation and migration during primary palate development. In *Current Research Trends in Prenatal Craniofacial Development* (ed. Pratt/Christiansen), pp. 119–132, Elsevier, North Holland, Inc.

MINKOFF, R. (1980*b*). Regional variation of cell proliferation within the facial processes of the chick embryo: a study of the role of 'merging' during development. *J. Embryol. exp. Morph.* **57**, 37–49.

MINKOFF, R. (1983). Distribution of gap junctions in mesenchyme during primary palate formation. *J. dent. Res.* **62**, 236.

MINKOFF, R. (1984). Cell cycle analysis of facial mesenchyme in the chick embryo: I. Labelled mitoses and continuous labelling studies. *J. Embryol. exp. Morph.* **81**, 49–59.

MINKOFF, R. (1990). Cell proliferation during formation of the embryonic facial primorida. *J. craniof. gen. dev. Biol.*, in press.

MINKOFF, R. AND KUNTZ, A. J. (1977). Cell proliferation during morphogenetic change; analysis of frontonasal morphogenesis in the chick embryo employing DNA labeling indices. *J. Embryol. exp. Morph.* **40**, 101–113.

MINKOFF, R. AND KUNTZ, A. J. (1978). Cell proliferation and cell density of mesenchyme in the maxillary process and adjacent regions during facial development in the chick embryo. *J. Embryol. exp. Morph.* **46**, 65–74.

MINKOFF, R. AND MARTIN, R. E. (1984). Cell cycle analysis of facial mesenchyme in the chick embryo: II. Label dilution studies and developmental fate of slow cycling cells. *J. Embryol. exp. Morph.* **81**, 61–73.

NAGY, J. I., YAMAMOTO, T., SHIOSAKA, S., DEWAR, K. M., WHITAKER, M. E. AND HERTZBERG, E. L. (1988). Immunohistochemical localization of gap junction protein in rat CNS: A preliminary account. In *Gap Junctions* (eds Hertzberg, E. L. and Johnson, R. G.) pp. 375–389 New York, Alan R. Liss.

NICHOLSON, B., DERMIETZEL, R., TEPLOW, D., TRAUB, O., WILLECKE, K. AND REVEL, J. P. (1987). Two homologous protein components of hepatic gap junctions. *Nature* **329**, 732–734.

PATTEN, B. M. (1968). *Human Embryology*. New York: McGraw-Hill.

PATTERSON, S. B., JOHNSTON, M. C. AND MINKOFF, R. (1984). An implant labeling technique employing sable hair probes as carriers for ^{3}H-thymidine: applications to the study of facial morphogenesis. *Anat. Rec.* **210**, 525–536.

PATTERSON, S. B. AND MINKOFF, R. (1985). Morphometric and autoradiographic analysis of frontonasal development in the chick embryo. *Anat. Rec.* **212**, 90–99.

PAUL, D. L. (1986). Molecular cloning of cDNA for rat liver gap junction protein. *J. Cell Biol.* **103**, 123–134.

REVEL, J. P. AND BROWN, S. S. (1976). Cell junctions in development, with particular reference to the neural tube. *Cold Spring Harbor Symp. quant. Biol.* **40**, 433–455.

ROMANOFF, A. L. (1960). *The Avian Embryo*. New York: Macmillan.

SABER, M., PARKER, S. B. AND MINKOFF, R. (1989). Influence of epithelial–mesenchymal interaction on the viability of facial mesenchyme *in vitro*. *Anat. Rec.* **225**, 56–66.

SAEZ, J. C., NAIRN, A. C., CZERNICK, A., SPRAY, D. C., HERTZBERG, E. L. AND BENNETT, M. V. L. (1990). Phosphorylation of connexin 32, a hepatocyte gap junction protein, by cAMP-dependent protein kinase, protein kinase C and Ca^{2+}/calmodulin-dependent protein kinase II. *Eur. J. Biochem.* (in press).

SCHOENWOLF, G. C. AND KELLEY, R. O. (1980). Characterization of intercellular junctions in the caudal portion of the developing neural tube of the chick embryo. *Am. J. Anat.* **158**, 29–41.

SCHWANTZEL-FUKUDA, M. AND PFAFF, D. W. (1989). Origin of luteinizing hormone-releasing hormone neurons. *Nature* **338**, 161–164.

SHIOSAKA, S., YAMAMOTO, T., HERTZBERG, E. L. AND NAGY, J. I. (1989). Gap junction protein in rat hippocampus: correlative light and electron microscope immunohistochemical localization. *J. comp. Neurol.* **281**, 282–297.

STREETER, G. L. (1948). Developmental horizons in human embryos. *Contr. Embryol. Carn. Instn. Washington* **32**, 133–203.

SWENSON, K. I., JORDAN, J. R., BEYER, E. C. AND PAUL, D. L. (1989). Formation of gap junctions by expression of connexins in *Xenopus* oocyte pairs. *Cell* **57**, 145–155.

WERNER, R., LEVINE, E., RABADAN DIEHL, C. AND DAHL, G. (1989). Formation of hybrid cell-cell channels. *Proc. natn. Acad. Sci. U.S.A.* **86**, 5380–5384.

WRAY, S., NIEBURGS, A. AND ELKABES, S. (1989). Spatiotemporal cell expression of luteinizing hormone-releasing hormone in the prenatal mouse: evidence for an embryonic origin in the olfactory placode. *Devl. Brain Res.* **46**, 309–318.

XU, Z., PARKER, S. B. AND MINKOFF, R. (1990). The influence of epithelial–mesenchymal interaction on the viability of facial mesenchyme II: Synthesis of basement membrane components during tissue recombination. *Anat. Rec.* **228**, 58–68.

YAMAMOTO, T., OCHALSKI, A., HERTZBERG, E. L. AND NAGY, J. I. (1990). LM and EM immunolocalization of the gap junctional protein connexin 43 in rat brain. *Brain. Res.* **508**, 313–319.

(*Accepted 22 October 1990*)